

Methane Absorption Variations in the Spectrum of Pluto

MARC W. BUIE¹ AND UWE FINK

Lunar and Planetary Laboratory, University of Arizona, Tucson, Arizona 85721

Received August 15, 1986; revised February 18, 1987

Absolute spectrophotometry of Pluto in the wavelength range of 5600 to 10,500 Å was obtained on 4 nights covering lightcurve phases of 0.18, 0.35, 0.49, and 0.98. The four phases included minimum light (0.98) and one near maximum light (0.49). The spectra reveal significant variations in the absorption depths of the methane bands at 6200, 7200, 7900, 8400, 8600, 8900, and 10,000 Å. The minimum amount of absorption was found to occur at minimum light. This variation would imply a 30% change in the column abundance of methane within 3 days. A model employing an anisotropic surface distribution of methane frost and a clear layer of CH₄ gas was developed to explain the variation in absorption strength with rotational phase. The fit to the overall spectrum requires the presence of a frost with particle sizes on the order of a few millimeters. An upper limit of 5.5 m-am is derived for the one-way column abundance of CH₄ gas. An equally good fit to the variation of the 7200-Å band is obtained if the atmosphere is removed from the model entirely. © 1987 Academic Press, Inc.

INTRODUCTION

Previous observations of Pluto have revealed a very interesting planet. Its orbit has the largest semimajor axis and eccentricity of any known planet in the Solar System. This gives it a perihelion distance of 29.6 AU and an aphelion distance of 49.3 AU, resulting in a large temperature variation during a Plutonian year.

Photoelectric observations of Pluto since 1953 (Walker and Hardie 1955, Hardie 1965, Andersson and Fix 1973, Neff *et al.* 1974, Binzel and Mulholland 1984, Tholen and Tedesco 1986) have shown that there are substantial brightness variations. Pluto's lightcurve has been observed to have a large amplitude varying from about 0.12 mag in 1955 to almost 0.3 mag today. In addition, the mean of the lightcurve has decreased by about 0.22 mag over the same period of time. Analyses of this photometry

have attributed the rotational lightcurve to surface albedo features (Lacis and Fix 1972, Marcialis 1983).

Infrared photometry by Cruikshank *et al.* (1976) and Cruikshank and Silvgaggio (1980), and spectroscopic studies by Fink *et al.* (1980), Soifer *et al.* (1980), and Apt *et al.* (1983) have shown the presence of methane. Both a methane atmosphere and surface frost have been called upon to explain the observed absorption features. Unfortunately, methane frost and gas display very similar spectra at medium to low resolution, and distinguishing between the two phases on the basis of absorption strength or band shape can be very difficult. Knowledge of the column abundance of CH₄ gas can give a direct determination of the surface temperature, a quantity that is difficult to measure with current infrared instruments.

A lightcurve of the CH₄ absorptions can furnish diagnostic information that can distinguish between gaseous and solid methane. If the absorption were due entirely to a uniform atmosphere, the equivalent width

¹ Present address: Institute for Astronomy, University of Hawaii, 2680 Woodlawn Dr. Honolulu, HI 96822.

of the bands should not change as Pluto rotates. A nonuniform covering of frost, on the other hand, would show a variation.

The objective of the research was to monitor the spectrum of Pluto as it rotates. The spectrograph described by Fink *et al.* (1980) was used for the new observations because it had demonstrated the ability to acquire spectra with good signal-to-noise ratios in a single night. With this instrument and the rotational period of Pluto of about 6 days it was possible to obtain high signal-to-noise spectra covering a range of lightcurve phases. The observations and modeling of spectra obtained at four different rotational phases are described in this paper.

OBSERVATIONS AND INSTRUMENTATION

All of the observations were carried out at the 155-cm Catalina Observatory telescope during the period 1983 April 18–23. A summary of the 61 exposures of Pluto from 4 nights is presented in Table I.

The transmission grating spectrograph used gave a resolution of about 20 Å in the wavelength range 0.56 to 1.05 μm. The image scale at the entrance slit was 10 arcsec mm⁻¹, yielding a field of view of 180" along the slit and 10" across the slit. A slit width of 10" was chosen so that essentially all of the light from Pluto could be collected, and so that absolute spectrophotometry could be carried out. The reduction of the beam by the final lens gave a scale of about 80 arcsec mm⁻¹ along the length of the slit and a dispersion of about 700 Å/mm.

TABLE I
SUMMARY OF OBSERVATIONS OF PLUTO

UT date	Number of exposures	Total time (min)	Rotational phase
1983 Apr 18	12	120	0.19
1983 Apr 19	20	200	0.35
1983 Apr 20	20	200	0.50
1983 Apr 23	9	90	0.97

Note. $r = 29.891$ AU, Pluto–Sun distance; $\Delta = 28.934$ AU, Earth–Pluto distance; $\alpha = 0.7^\circ$, phase angle between the Earth and the Sun as seen from Pluto.

The detector employed for all of the observations was an 800 × 800 charge coupled device (CCD) array of 15-μm pixels manufactured by Texas Instruments for the Space Telescope camera. The CCD and its associated readout electronics were used in cooperation with the Space Telescope Wide Field Planetary Camera investigation definition team.²

During the observations special care was taken to track the object accurately during integrations, the longest of which was 10 min. To allow corrections for telluric absorptions observations of SAO 120312, a G5 star, were interposed between exposures of Pluto. This regular sampling of a comparison star throughout the night also made it possible to determine extinction coefficients for each night, necessary for calibrating SAO 120312 with respect to the standard stars. As well as monitoring air mass effects, this procedure monitored slow seeing changes that affect the amplitude of the channel fringes (see next section). SAO 120312 was chosen for its proximity to Pluto, similarity in color to the Sun, and its relatively low brightness level ($M_v = 9.2$). The latter allowed long enough exposures (~25 sec) to average out seeing fluctuations so that spectra of the comparison star were of seeing disk averages and thus comparable to Pluto.

DATA REDUCTION

The process of data reduction is largely unchanged from that described by Fink *et al.* (1980) and Johnson *et al.* (1984). A few new steps have been added to the reductions to achieve the highest possible signal-to-noise. These steps are (1) removal of cosmic ray strikes on each raw image, (2) dividing all data by a flat-field, and (3) shifting of individual spectra by a fraction of a pixel to line up instrumental and telluric features between the spectra to a high degree of precision.

² Team members are W. B. Baum, A. D. Code, D. G. Currie, G. E. Danielson, J. E. Gunn, T. Kelsall, J. Kristian, C. R. Lynds, P. K. Seidelman, B. A. Smith, and J. A. Westphal.

For accurate spectrophotometry summing all the signal was considered to be a primary objective. In this case the summation aperture along the slit for the object signal should be as large as possible to ensure that all of the light is collected. Such a large aperture degrades the signal-to-noise ratio by including too much sky signal along with the light from the object. The optimum signal-to-noise in this case is achieved with an object aperture of 5 pixels (Buie 1984). For this data set an aperture of 9 pixels (~ 15 arcsec) was chosen to ensure the complete summation of the signal while retaining most ($\sim 90\%$) of the possible signal-to-noise. The same aperture was also used for the comparison star so that any fractional loss was equal for the two.

Wavelength calibration of the data was carried out with exposures of a helium emission lamp. The dispersion determined from a linear least-squares fit was $10.60 \text{ \AA}/\text{pixel}$. To obtain a precise wavelength scale ($\pm 15 \text{ \AA}$) the position of a telluric absorption, the oxygen A-band (O_2A) at 7260 \AA , was used as a reference point for each spectrum.

A complete description of the techniques used for cosmic ray strike removal is given by Buie (1984). Flat-field corrections were provided by dividing each raw CCD image by a high signal-to-noise image (uniform along the slit) taken of the telescope dome. In any case only a small correction was introduced by the flat-fielding process because all objects were positioned on the same place in the slit.

Figure 1 shows a raw spectrum of the comparison star using a 1-mm slit. Traces from several different flat-fields at a variety of slit widths are also shown. The sinusoidal fluctuations, or channel fringes, are the result of optical interference between the front and back surfaces of the relatively thin (about $16 \mu\text{m}$) absorbing silicon layer of the CCD. The amplitude of the channel fringes is determined by the spectral resolution, as shown in the flat-field curves. In the case of point sources the spectral resolution was not defined by the slit, but

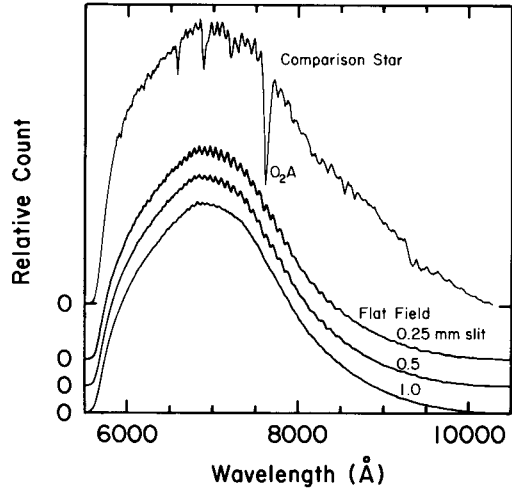


FIG. 1. Top curve is a raw spectrum of SAO 120312 that was used as the reference spectrum for shifting. Below are traces of the same row from three flat fields recorded with different slit widths. The top, middle, and bottom curves correspond to 0.25-, 0.5-, and 1-mm slit widths, respectively. Note the increase in the fringe amplitude with increasing spectral resolution.

by the size of the seeing disk for each exposure.

The exact placement of the channel fringes on the detector was determined by the object's position in the entrance slit. Centering within the entrance slit was accurate to within $\sim 1''\text{--}3''$, resulting in random shifts of the spectra and their interference fringes by 1–2 pixels in the focal plane of the array. Additional noise is introduced into the data if this misregistration between different exposures is not corrected.

Shifting of the spectra was accomplished by a convolution of the data with a shifted sinc function which preserves all of the information (i.e., lineshapes and even noise) in the data. The foundations for this process are explained in Bracewell (1965), and a detailed description of its usage for these reductions can be found in Buie (1984).

With this approach all of the spectra were registered with respect to the stellar reference spectrum shown in Fig. 1. The optimum shift was determined by minimizing the noise in the ratio of the unknown spectrum and the reference. The result of this

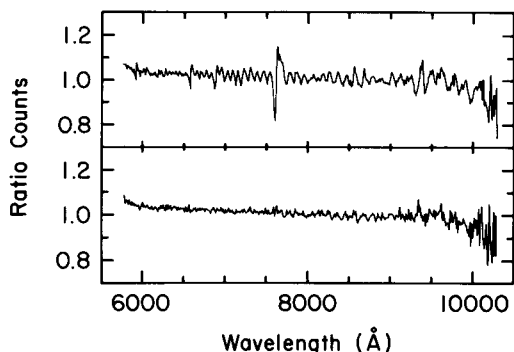


FIG. 2. Ratio of two different exposures of the same comparison star taken on the night of 1983 April 23 shown with no shifting on the top and a relative shift of 0.877 pixels on the bottom.

procedure is illustrated in Fig. 2. When the two spectra are not registered the ratio is very noisy due to the mismatch in the channel fringes while the strong telluric absorptions, such as the O_2A band, show a characteristic "S" shape pattern. After shifting, the fringes and "S" shapes disappear. The shifts required ranged from no shift to 2 pixels, with the average shift being about 0.5 pixels.

This technique does not guarantee perfect cancellation of the telluric absorptions and channel fringes. The telluric features are only canceled when the air mass is well matched and atmospheric absorbers such as water vapor are constant throughout the night. Similarly, changes in seeing during the night will prevent good cancellation of the interference fringes, because of the varying spectral resolution. The effects of these problems were minimized with frequent and periodic observations of comparison stars.

Only after the spectra were registered with respect to the reference spectrum could they be averaged. For each night all of the Pluto spectra were averaged with equal weight. The comparison star average was constructed by using all available exposures from that night. If the resulting mean air mass was not identical to that of Pluto, one or two comparison star spectra were removed from the average to make the match as close as possible.

The average of the Pluto spectra for 4 nights is illustrated in Fig. 3, where the data from this investigation are compared to the previous spectrum by Fink *et al.* (1980). Both are plotted on a relative reflectance scale normalized to 1 at 6000 Å. The slight difference in slope is due to the different comparison stars used. Aside from the obvious improvement in the signal-to-noise, the spectra are quite similar except that the shape of the 8900-Å band has changed since 1980. A discussion of the implications of this change will follow in the conclusions.

Absolute flux calibration of the spectra require correcting for atmospheric extinction. The extinction coefficients were determined from the comparison star spectra for each night by a least-squares fit to each wavelength and are shown in Fig. 4.

While the variation in opacity caused by the changing amounts of atmospheric water vapor from night to night is expected, the changes in the extinction at the short-wavelength end of the spectrum is not readily explained. It is possible that this is due to varying amounts of volcanic dust from the eruption of El Chichon in 1982. These data demonstrate the need for caution in the use of "average" extinction coefficients for a given site. The data plotted in Fig. 4 demonstrate that for the best results the extinction must be determined every night.

The final phase of the data reduction procedure involved determination of the abso-

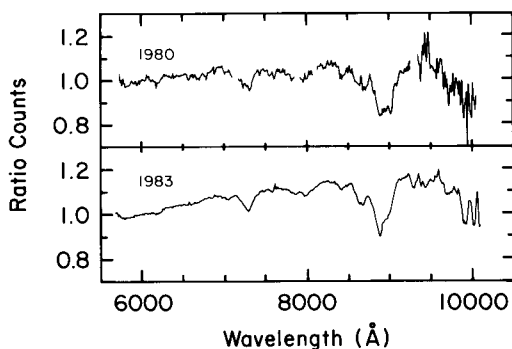


FIG. 3. Average of all four Pluto-SAO 120312 ratios for 1983 compared with the data from Fink *et al.* (1980). The 1983 data represents 470 min of integration on Pluto while the 1980 data represents only 35 min.

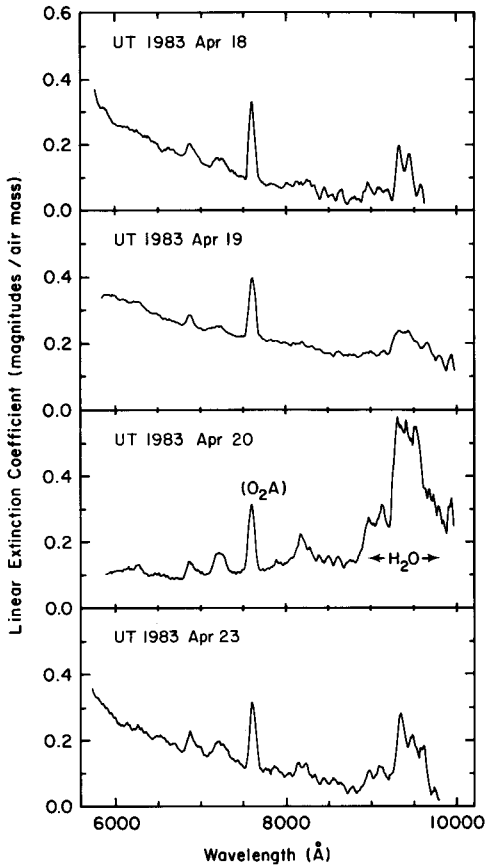


FIG. 4. Extinction curves for 1983 April 18, 19, 20, and 23 (top to bottom).

lute flux and geometric albedo for Pluto. Absolute calibration of the spectra for each individual night was carried out by observing the standard stars 109 Vir and BS 6629 for which absolute flux levels have been published by Johnson (1980).

The 10" entrance slit of the spectrometer was wide enough (Johnson *et al.* 1984) to admit all the light so that no correction for the light lost outside the slit was required. Since the ratios of comparison star/standard star and Pluto/SAO 120312 were smoothly varying, four points of the spectrum sufficed for calibration purposes. The points were chosen to avoid telluric absorptions and methane features in Pluto's spectrum. At each wavelength the number of counts per second was determined from an average of 15 adjacent points in the spec-

TABLE II
ABSOLUTE CALIBRATION OF SAO 120312^a

Date (UT)	Standard star	Wavelength (Å)			
		6000	7000	8000	9500
18 Apr 1983	109 Vir	5.85	4.61	3.74	3.21
18 Apr 1983	109 Vir	5.84	4.60	3.68	3.12
19 Apr 1983	109 Vir	5.94	4.66	3.76	3.25
19 Apr 1983	109 Vir	5.69	4.54	3.64	3.07
20 Apr 1983	109 Vir	6.25	4.88	3.87	3.27
20 Apr 1983	109 Vir	6.05	4.82	3.89	3.39
23 Apr 1983	BS 6629	5.52	4.48	3.67	2.87
Average		5.88	4.66	3.75	3.17
σ of the mean		0.09	0.06	0.004	0.06

Note. Pairs of values for a particular date refer to measurement before and after transit of the star.

^a Flux ($\text{erg cm}^{-2} \text{sec}^{-1} \text{Å}^{-1}$) $\times 10^{13}$

trum. Multiplying the measured count ratio by the absolute flux of the standard yielded the absolute flux of the comparison star. The air mass correction was then applied from the previously determined extinction coefficients. This correction was generally about 1% with the largest being 5%. For each night the absolute flux of the comparison star was calculated independently. For the final absolute flux determination of the star SAO 120312 the average was taken and is shown at the bottom of Table II. Table III gives the absolute flux determination of Pluto for each of the 4 nights of observation.

The errors shown for the absolute calibration are the random errors from all of the independent calibrations. A referee for this paper has noted that the single calibration based upon BS 6629 appears to be sys-

TABLE III
ABSOLUTE CALIBRATION OF PLUTO^a

Date (UT)	Phase	Wavelength (Å)			
		6000	7000	8000	9500
18 Apr 1983	0.19	10.4	8.87	7.21	6.33
19 Apr 1983	0.35	10.5	8.93	7.31	6.51
20 Apr 1983	0.48	11.0	9.27	7.60	6.64
23 Apr 1983	0.98	9.14	7.83	6.52	5.78

^a Flux ($\text{ergs cm}^{-2} \text{sec}^{-1} \text{Å}^{-1}$) $\times 10^{15}$.

tematically below the mean, indicating that systematic errors dominate over random errors. The calibration of SAO 120312 based on BS 6629 and 109 Vir differ by $\sim 7\%$.

To derive the geometric albedo it is necessary to divide the flux spectrum of Pluto by the incident solar flux. An approximate method is to use a solar-type comparison star whose flux spectrum is very nearly the same as that of the Sun. The comparison star SAO 120312 is classified in the SAO catalog as a G5 star, and upon comparing its flux spectrum to that of the Sun (Arvsen *et al.* 1969) it was found to have the same color as the Sun to within the accuracy of our data, that is, about 1%. Therefore the geometric albedo of Pluto can be determined directly to within this error from the ratio spectrum.

For the absolute scaling of the geometric albedo only one wavelength, chosen to be 6000 Å, is required. It should be noted that the derived geometric albedo spectrum is for Pluto and Charon seen together. The relative contribution of Charon to the total flux is not precisely known now and may not be constant. The relative flux contributions of Charon needs to be taken into account in any modeling. Table IV contains a summary of physical parameters adopted for the Pluto-Charon system.

The uncertain quantities in the geometric albedo calibration are (1) flux of the Sun (good to $\sim 3\%$), (2) flux of Pluto-Charon (good to $\sim 10\%$), and (3) projected areas of Pluto and Charon (good to $\sim 50\%$). The uncertainties in r and Δ are negligible. The importance of the large uncertainty in the area of Pluto and Charon is lessened by including the radii in the model calculation.

The final observational results of this investigation are displayed in Fig. 5. The figure shows the geometric albedo spectrum of Pluto for rotational phases 0.19, 0.35, 0.49, and 0.98. Methane absorption bands at 6200, 7200, 7900, 8400, 8600, 8900, and 10,000 Å are clearly evident in all the spectra. The strongest band in the spectrum is at

TABLE IV
ADOPTED PHYSICAL PARAMETERS OF PLUTO
AND CHARON

Pluto mass	$M = 1.4 \times 10^{25}$ g
Pluto radius	$R = 1500$ km
Charon mass	$m = 1.8 \times 10^{24}$ g
Charon radius	$r = 750$ km
Charon-Pluto separation	20,000 km
Pluto surface gravity	$g = 41.5$ cm sec $^{-2}$
Pluto-Charon density	$\rho = 1$ g cm $^{-3}$
Charon orbital period	Same as lightcurve
First minimum light in 1980	JD 2444240.661
Lighttime correction	0.167 day
Lightcurve period	6.38726 days

Note. Parameters are from various sources: Trafton and Stern (1983), Hege *et al.* (1982), and Tholen and Tedesco (1986). The flux assumed for the Sun is from Arvsen *et al.* (1969). The values for r and Δ at the time of the observations are listed in Table I.

8900 Å. It can easily be seen on the spectra for phases 0.49 and 0.98 that the depths of the methane absorption features are different. The overall change in brightness for the various phases agrees with that expected from the lightcurve.

The 10,000-Å feature is noisy because it appears at the edge of sensitivity of the instrument and is not clearly defined, but definitely seems to be present. Appearing next to the 8900-Å band are two shoulders at 8400 and 8600 Å. At 7900 Å is a weak shallow band that is very useful for fitting the column abundance of the atmosphere and constraining the frost model. A very well-defined band with a good signal-to-noise ratio is located at 7200 Å, and is important in the subsequent model analyses. The weakest feature, at 6200 Å, is not seen clearly at all phases, but seems to be present. On no spectrum is this feature as strong as seen in the data from Fink *et al.* (1980).

ANALYSIS

Explaining the observed spectrum depends upon the behavior of methane frost and methane gas under conditions likely to exist on Pluto. A synthetic match to the Pluto spectrum has already been published

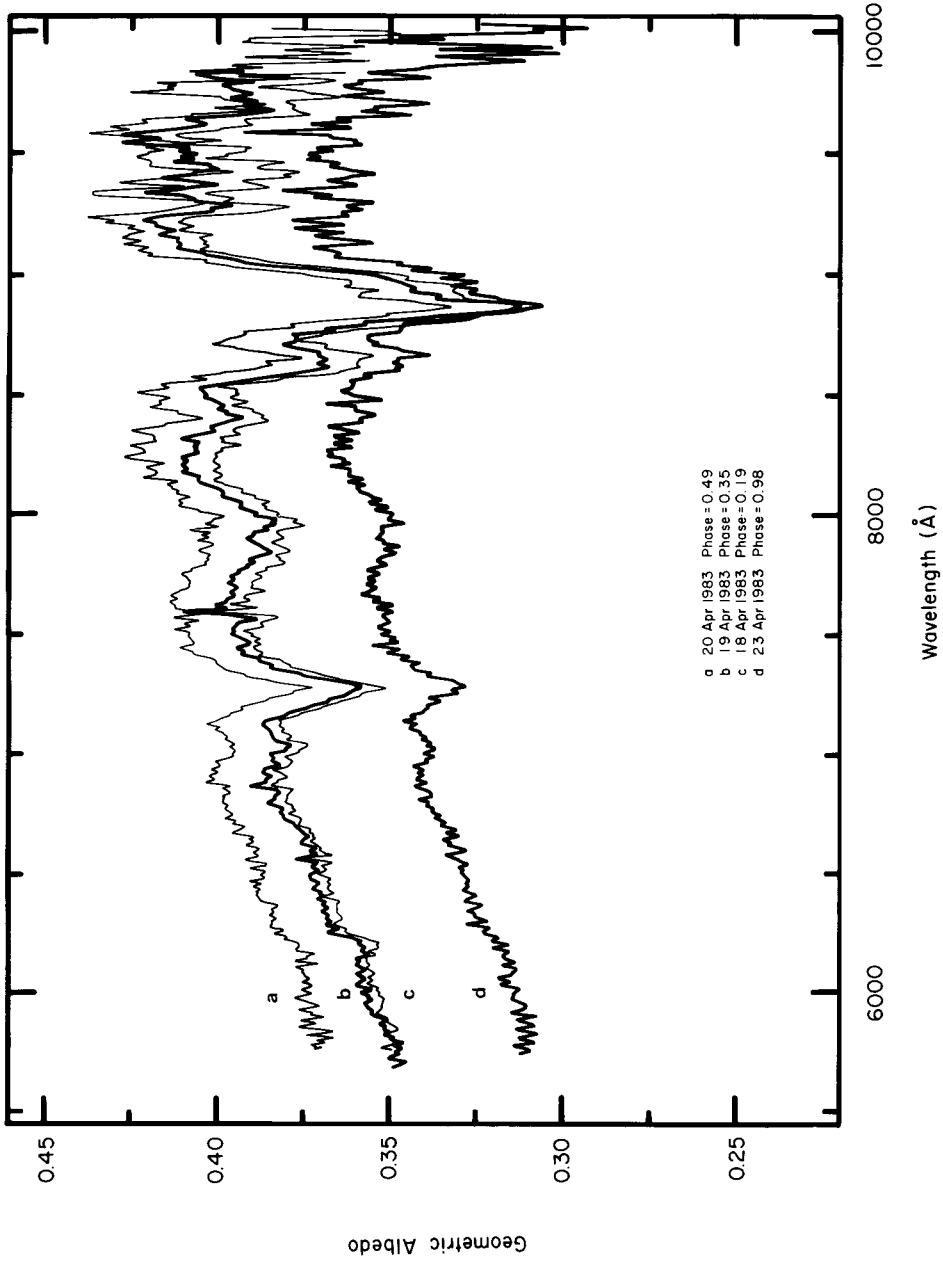


FIG. 5. Geometric albedo of Pluto-Charon for 1983 April 18, 19, 20, and 23. These correspond to rotational phases 0.19, 0.35, 0.49, and 0.98, respectively. The range of geometric albedo displayed was chosen to exhibit both the spectral features and the noise level on a reasonable scale. Two spectra (phases 0.19 and 0.35) exhibit slightly imperfect cancellation of the telluric absorptions which is attributed to changing atmospheric conditions during those 2 nights.

for methane gas (Fink *et al.* 1980) but little has been done for methane frost.

The data in Fig. 5 clearly show that the depths of the methane features are dependent on rotational phase. Every band of methane observed was weakest at the phase corresponding to minimum light (0.98). There was a perceptible change even between the phases of 0.35 and 0.49. For a uniform amount of gaseous methane the total amount of absorption would remain nearly constant with rotational phase. Some variation would be expected for an inhomogeneous surface because the albedo pattern will change the column abundance integrated over the disk. If the center of the disk is darker than the area near the limb, the high air mass regions are weighted more in the integral. The absorption depth would be larger for this case than for a uniform sphere. If Pluto's lightcurve minimum is caused by a dark spot on the center of the disk (e.g., Marcialis 1983) then the absorption due to the gas would be greatest at minimum light. This is opposite to what is observed. Thus the data present evidence that at least a fraction of the methane absorption observed is due to a surface frost layer which is nonuniformly distributed over the surface of Pluto.

(a) Photometric Spot Model

The photometric lightcurve of Pluto combined with the large obliquity of the rotational axis can lead to a detailed model of the surface albedo distribution. One such model was constructed successfully for Saturn's satellite, Iapetus (Morrison *et al.* 1975), as verified by the Voyager imaging results (Smith *et al.* 1982). Marcialis (1983) has developed a model that attempts to explain the known variation of Pluto's lightcurve in which he uses two circular dark areas on the surface to explain the changing amplitude and shape of the lightcurve since 1955. However, this model was not able to account for the decrease in Pluto's mean brightness. This secular dimming might be

explained by a more complicated surface albedo distribution, including polar caps or bands, or it might be explained by physical changes of Pluto's surface properties such as the evaporation of ices, which might result from Pluto's changing distance from the Sun.

From these considerations the simple two-spot model cannot be expected to lead to a complete interpretation of the spectroscopic data. Nonetheless it is a physically reasonable model that can be used as a starting point to constrain two different types of terrain with different optical properties.

The relevant parameters from the two-spot model developed by Marcialis are the spot sizes and locations. The latitudes of both spots are 23°S, while their radii are 46° and 28° at west longitudes of 0° and 134°, respectively. The longitude used here increases with time and is referenced to 0° long at minimum light (lightcurve phase = 0). Note that the direction of Pluto's north pole has been defined in accord with the right-hand rule for spin vectors in physics (i.e., choice 'c' from Davies *et al.* (1980, p. 215)) which is different from the adopted IAU convention). In 1983 the sub-Earth point was ~10° south of Pluto's equator and moving north by about 2.2° per year. The spots were used as a starting point to constrain the distribution of methane on Pluto. The contrast ratio and limb darkening are determined in the current treatment.

(b) Synthetic Frost Calculations

A rigorous solution to the general scattering problem of a closely packed surface frost with arbitrary particle shapes has not yet been achieved. Hapke (1981) details an approach for the approximate calculation of a spectrum for multiply scattering, close packed surface particles given sufficient knowledge of their composition.

The first step in the Hapke model calculation is to determine the average single scattering albedo from the complex index of re-

fraction and particle size of a material. The material on Pluto's surface is assumed to be methane frost. The real part of the index of refraction for methane is $n_r = 1.33$ (Marcoux 1969) and was assumed to be constant from 5000 to 10,000 Å. The imaginary index of refraction can be calculated from the absorption coefficient for the particles as a function of wavelength. Imaginary indices are not available in the literature for solid methane, but optical depths for liquid methane have been reported by Ramaprasad *et al.* (1978). These were converted to imaginary indices. The absorption coefficients for the liquid agree quite closely to those for the gas (e.g., Fink *et al.* 1977). Since the difference in density between solid and liquid methane is much smaller, the approximation should be quite good for this resolution. The value determined for the liquid will be used in the subsequent analysis.

The geometric albedo as a function of wavelength can then be calculated leaving only the particle size as a free parameter. The conditions under which Hapke's theory is valid (as applied here) are (1) particle size is much larger than the wavelength of light, (2) particles are closely packed, (3) particles are irregularly shaped, and (4) a surface integration element consists of a homogeneous mixture of a single type of particle.

The dependence of the synthetic spectrum on the particle's phase function was explored. The depth of the absorptions was not found to be critically dependent on the phase function chosen. The actual function for Pluto's surface particles is not known, but a reasonable approximation is the isotropic case. Throughout the rest of the analyses this case is assumed.

Using the absorption coefficients of Ramaprasad for methane it is not possible to match the observed wavelength variation of Pluto's continuum, and material having a wavelength-dependent absorption coefficient must be added. An easy way to fit the observed spectrum is to modify the equation for optical depth given in Hapke

(1981). The new equation becomes

$$\tau(\lambda) = \alpha(\lambda)D_e + \tau_0(\lambda), \quad (1)$$

where the first term represents the opacity due to methane and the last term is the optical depth due to other absorbing material in the particle. The latter is considered to be the continuum optical depth. This treatment has the advantage that τ_0 can be determined independent of the particle size, thus separating the task of fitting the continuum albedo and the depths of the methane bands.

The calculation of the complete model required a numerical integration over the visible hemisphere. Four parameters needed to be specified: the particle size and τ_0 for the area within the spots and for the area outside of the spot boundaries. To perform the integration the surface was broken up into annuli about the center of the apparent disk. The contribution to the integral for each annulus is the weighted average of the integrand evaluated for each terrain type, and the weights are equal to the fraction of the annulus covered by each type. The integral was evaluated using the Gaussian quadrature mesh points tabulated in Stroud and Secrest (1966) for a 40-point sum.

The spectra shown in Fig. 5 represent the geometric albedo of Pluto and Charon together. The light from Charon was modeled by assuming it to be a uniform sphere with no methane on its surface. Thus the geometric albedo of Charon is determined by the value of τ_0 chosen for its surface, adding a fifth free parameter to the model.

The first step in fitting the model to the data is to adjust the continuum level. The value of τ_0 must be determined for the two terrain types on Pluto and for Charon yielding three unknowns at each wavelength. Since each wavelength has been measured at four different rotational phases, three continuum parameters can in principle be determined. Since Charon only contributes roughly 20% of the flux, the model is not very sensitive to the value chosen for its τ_0 . For this reason τ_0 for Charon was arbitrarily

constrained to be somewhere between the τ_0 's for the bright and dark regions on Pluto. This now requires only two rotational phases to determine the two τ_0 's for Pluto.

To simplify the search for a solution five points in the continuum were picked across the spectrum at 6000, 6600, 7600, 8200, and 9360 Å. The spectra from opposite hemispheres, phases 0.49 and 0.98, were used to constrain the model. To simplify the following description bright (τ or radius) will refer to that quantity for the background material on Pluto. Dark will refer to the material interior to the spots.

The continuum optical depth as a function of wavelength, $\tau_0(\lambda)$, was specified by

$$\tau_0(\lambda) = a\lambda^2 + b\lambda + c. \quad (2)$$

The coefficients (a , b , and c) were determined from a least-squares fit to the τ_0 's for five chosen points across the spectrum. The

TABLE V

	CONTINUUM	OPTICAL DEPTH	QUADRATIC
	COEFFICIENTS		
	Bright areas on Pluto	Dark areas on Pluto	Charon
a	2.641×10^{-9}	1.936×10^{-8}	0
b	-4.763×10^{-5}	3.414×10^{-4}	1.143×10^{-5}
c	2.543×10^{-1}	1.659	2.290×10^{-1}

coefficients that were used for the rest of the analyses are listed in Table V.

Once the continuum is determined in the model, the methane bands can be investigated. The methane particle sizes that would match the absorptions were determined by fitting only the center of the 7200-Å band for the two phases. The best fit to the observed spectra is shown in Fig. 6 for

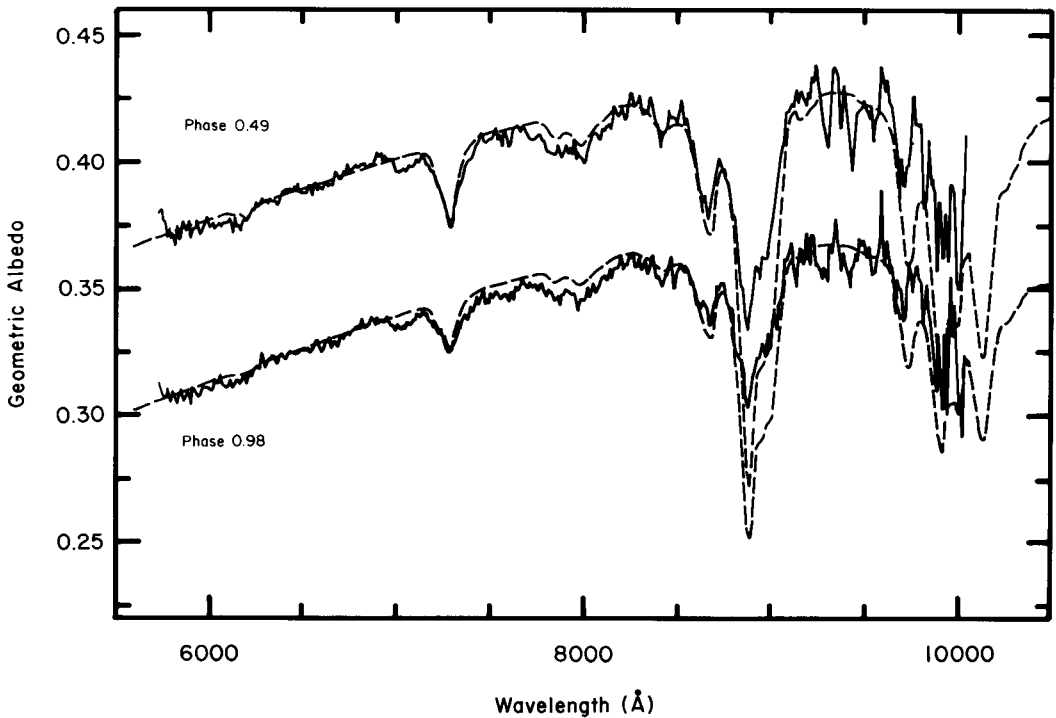


FIG. 6. Pure frost synthetic spectrum fitted to the 7290-Å band. This synthetic spectrum represents the best fit to the data that could be obtained with a pure frost model. Particle radii are 4.4 and 6.2 mm for the bright and dark areas, respectively. The solid lines are the data and the dotted lines are the calculated curves.

particle radii of 4.4 and 6.2 mm for the bright and dark areas, respectively. The model accurately reproduces the phase-dependent behavior of the 7200-Å band. The fit to the other methane bands is also quite good, with the exception of the 8900-Å band. This points out a shortcoming of the model in that the weak bands are too weak, or the strong bands are too strong. Multiple scattering in the frost has not enhanced the weak bands enough.

(c) Synthetic Gas Calculations

To include the behavior of an atmosphere over a spotted frost-free surface the continuum is fitted with the same parameters determined in the previous section while the effect of the atmosphere is included by multiplying by its transmission for each surface element. The transmission to a point on the surface as a function of μ ($\mu = \cos \theta$, where θ is the angle to the surface normal) is given by

$$T = \exp[-\tau(A)] \quad (3)$$

$$A = 2A_1/\mu,$$

where $\tau(A)$ is the mean optical depth of the atmosphere as a function of abundance, A is the slant path two-way abundance, and A_1 is the one-way column abundance along the normal to the surface (i.e., unit air mass). All column abundances reported will be given in terms of this quantity.

The procedure for calculating the mean optical depth of methane gas has been discussed in detail by Fink *et al.* (1977) and Benner (1979). They describe the use of the Mayer–Goody or random band model with a Lorentz lineshape. However, for the conditions that exist on Pluto ($T = 40\text{--}60^\circ\text{K}$ and $P \sim 10^{-5}$ atm) the ratio of the Doppler width to the Lorentz width is $\sim 10^3$. Voigt profiles were calculated by Fink *et al.* (1980) but were not found to be different from the pure Doppler case until pressures of ~ 0.05 atm were reached. Calculating a Voigt profile instead of a pure Doppler pro-

file involves computing one more embedded integral. This increase in complexity was not felt to be justified in light of the small correction it would provide. Furthermore, neglecting Lorentz broadening is an approximation that will not change the rotational phase-dependent behavior of the model.

The temperature used for the gas was determined from assuming equilibrium between the methane vapor pressure and atmospheric surface pressure. Over the range of column abundances investigated the equilibrium temperature falls in the range of 50 to 60°K. The transmission of the atmosphere is weakly dependent on the temperature, through its effect on the Doppler half-width so the actual value is not critical.

The methane gas absorption coefficients used in the band model calculations are from long-path methane absorption spectra from Fink *et al.* (1977) and Benner (1979). These absorption coefficients were determined at room temperature ($\sim 300^\circ\text{K}$) for Lorentz broadened lines. The mean line spacing (δ) for each band was also determined at room temperature and must be extrapolated to the conditions on Pluto. The constant value of $\delta = 0.1 \text{ cm}^{-1}$ was chosen because it is similar to values that Fink *et al.* (1980) used and yielded synthetic spectra that matched the appearance of Pluto's spectrum (cf. Fig. 7). For most of the observed bands at these abundances, a constant line spacing is a reasonable approximation. However, an even better fit is obtained by adjusting δ for each band (Fink *et al.* 1980). While the fit would be improved by this adjustment, the fit is not more significant since each δ adds an additional free parameter to the model calculation.

Figure 7 shows a synthetic spectrum with a column abundance of 9.4 m-am that matches the depth of the 7290-Å band for the rotational phase of 0.98. For the other hemisphere (phase = 0.49) 14.6 m-am is required to fit the band. The gas model cannot explain the phase dependence of the ab-

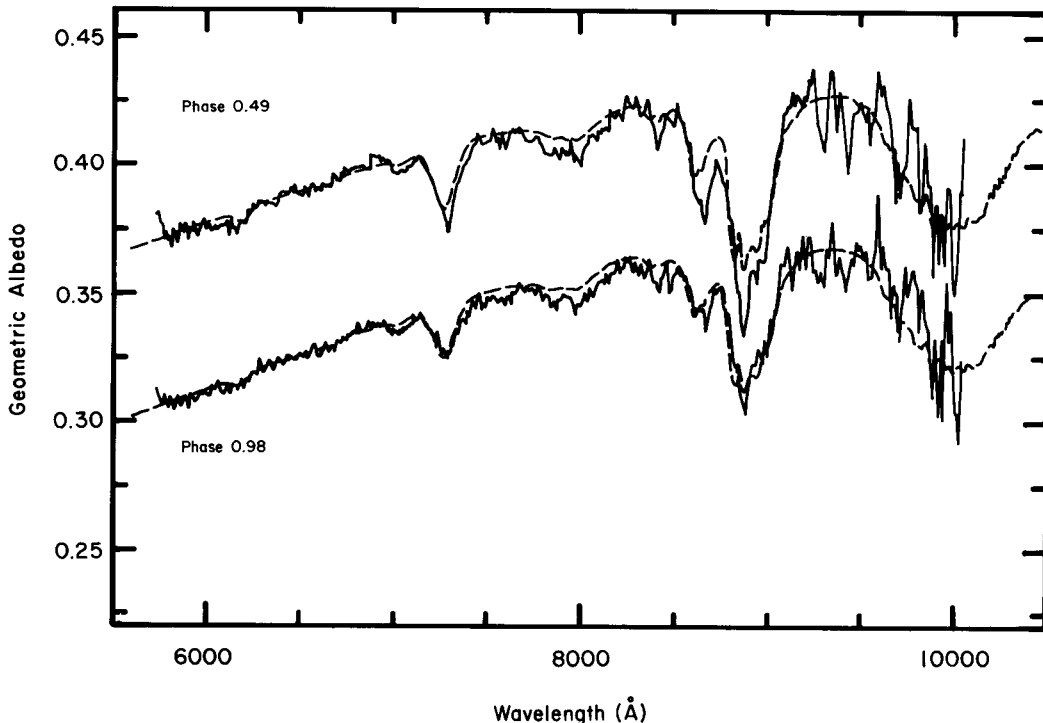


FIG. 7. Pure gas synthetic spectrum fitted to the phase 0.98. This synthetic spectrum represents an atmospheric fit to the data constrained by the 7290-Å band at a rotational phase of 0.98. The column abundance is 9.4 m-am.

sorptions. Trafton and Stern have investigated the properties of a methane atmosphere on Pluto (Trafton 1980, Trafton and Stern 1983, Stern and Trafton 1984). They conclude that Pluto's atmosphere would be in hydrostatic equilibrium and that there are no appreciable tides in the atmosphere for atmospheric densities considered here. Those arguments rule out variability in the atmosphere as the cause of the observed variations. Other explanations such as large systematic and long-lived cloud patterns cannot be ruled out, but there is no compelling evidence at this time to think this is likely. Thus it seems a surface frost distribution is a more reasonable explanation for the observed phase variation of the spectrum of Pluto.

(d) Final Model

The gaseous and solid methane absorptions calculated previously were combined. An upper limit to the gas abundance is found from the spectrum showing the mini-

um absorption (phase of 0.98). A value of 9.4 m-am was found under the fitting assumptions described above (see Fig. 7). A more realistic upper limit can be obtained from a model that combines gas and frost. The fit to the continuum is identical to that calculated in the individual models. There are now three parameters available to specify the methane absorptions: particle sizes

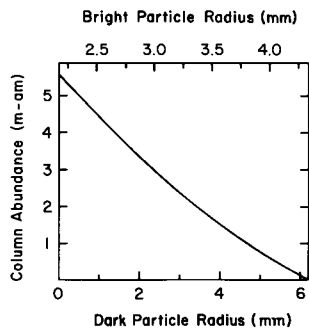


FIG. 8. The line represents the values of the three parameters that yield a match to the observed depth of the 7290-Å band in the phase 0.49 and 0.98 spectra.

in the two terrains on Pluto and the column abundance of the gas. The possible values of the three free parameters that yield a match to the depths of the 7290-Å band are shown in Fig. 8. The upper limit to the atmosphere is found when there is no methane frost left in the dark areas. For the present model calculations the upper limit is 5.6 m-am. Note that the bright particles are not necessarily bigger than the dark particles. In fact, there is a solution where the particles are the same size.

Figures 9 and 10 show the model fit for two selected possible solutions of the parameters plotted in Fig. 8. Figure 9 shows the fit at the gaseous upper limit, where the dark particle size is 0. Figure 10 is an intermediate case where the column abundance is 3 m-am and the particle diameters are 6.1 and 4.7 μm for the bright and dark areas, respectively. The case where the gas abundance is 0 was shown previously in Fig. 6. All three cases fit the 7200-Å band equally well, though the fit to the 8900-Å band is not the same for all. When the gas contribu-

tion is large, the relative band intensities are more reasonable, as would be expected. However, in no case is the fit to the phase variation of the 8900-Å band as good as for the 7200-Å band.

CONCLUSIONS

Methane absorption features in the spectrum of Pluto are shown to vary with rotational phase. A uniform atmosphere cannot explain this variation. A surface distribution of methane frost with or without an atmosphere is capable of explaining the rotational phase variation.

An upper limit to the gaseous column abundance assuming no frost contribution to the spectrum is 9.4 m-am. This number can be increased if the weaker bands in the spectrum are fitted at the expense of the stronger ones or if an atmospheric model with varying line spacing is used (e.g., Fink *et al.* 1980). If the spot model with frost is used and no solid methane is allowed in the dark regions, the present model assumptions give an upper limit of 5.4 m-am. The

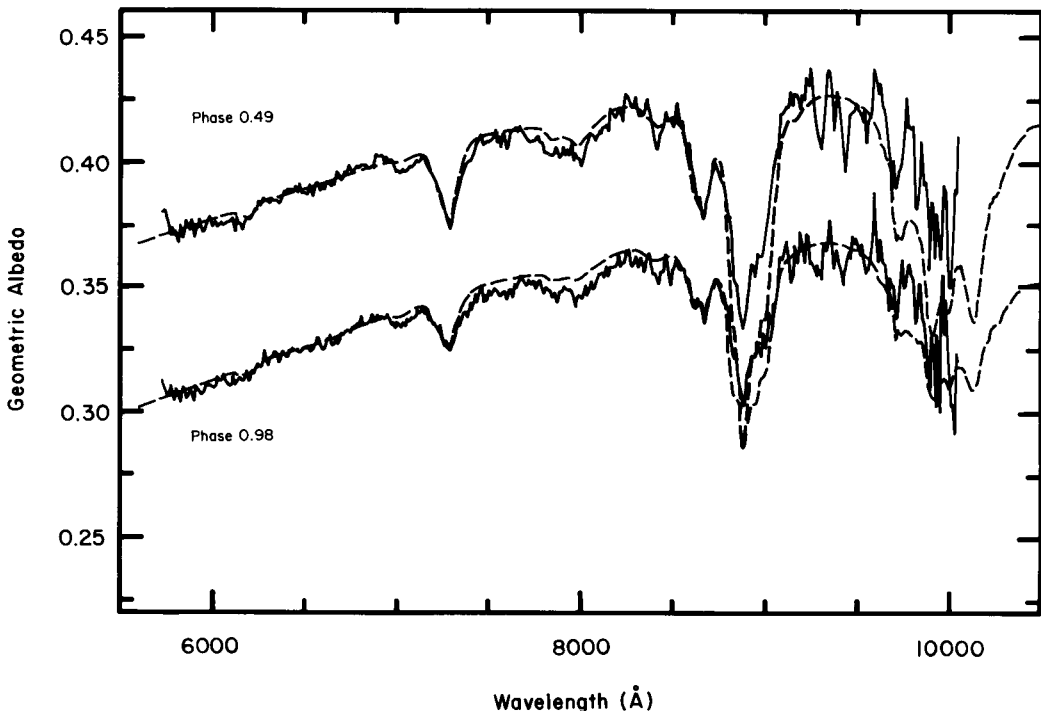


FIG. 9. Gas and frost model fit at the gas upper limit. Model fit for the point from Fig. 8 for dark particle size of zero. Column abundance of gas is 5.6 m-am and the bright particle radius is 2.2 μm .

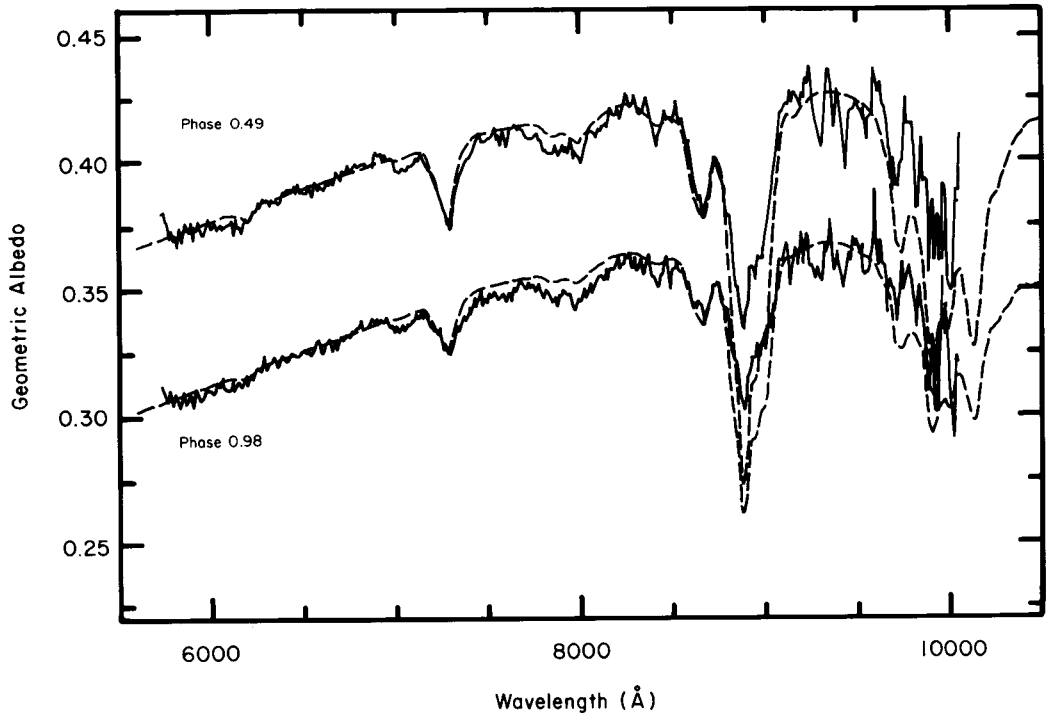


FIG. 10. Gas and frost model fit at a midrange solution. Model fit for a column abundance of 3 m-am, bright particle radius of 3.1 mm, and a dark particle radius of 2.4 mm.

column abundance derived from the model also depends on the light contributed by Charon. Since the satellite is assumed to be void of methane gas and frost, it represents a neutral component that reduces the absorption depth for a given column abundance. If methane frost exists on the surface of Charon, the derived methane column abundance would decrease.

The model of Pluto presented in this work includes albedo variations and a distribution of methane frost along with an atmosphere of methane gas. The model can explain the rotational phase variation of the methane features. The frost particles are as large as 6 mm if the atmosphere does not contribute to the methane absorptions, with smaller sizes required depending upon the bulk of the atmosphere (see Fig. 8). The numbers derived from the model depend on the choices made for the phase function and Charon's contribution to the total light. Changing these parameters will affect the derived particle sizes and the column abun-

dance, but not the general appearance and behavior of the synthetic spectra.

It is interesting to note that if albedo (thus temperature) controls the surface distribution of methane, less methane would be expected in the darker regions. This would lead to the sense of the variation that is seen. This correlation implies that the surface is not isothermal as suggested by Stern and Trafton (1984). Their model requires a minimum of ~ 3 cm-am of methane to maintain an isothermal atmosphere. This is considerably less than the upper limit of 5 m-am derived from this model. An observation that seems to run counter to the albedo-methane correlation is the behavior of the model for low gas abundances. As the column abundance of the gas goes to zero the particle size increases in the dark regions (see Fig. 8). The model does *not* imply less methane in the dark regions, only that the particles must be larger than in the bright regions if there is no atmosphere. Perhaps laboratory studies of the growth of

frost grains at these temperatures could support or refute this explanation.

A major problem with the model is its failure to reproduce the relative band strengths between the 7290- and 8900-Å bands. The frost is assumed to consist of a single particle size within a given terrain. The failure of the model to explain all of the methane features simultaneously might be explained by a more complex frost on the surface of Pluto. Clark and Roush (1984) have shown that a two-component frost (i.e., two particles sizes) will reduce the band ratio between weak and strong features. Another possible model that might yield a better fit is one that separates the continuum absorber and the methane frost. If the two components are separated on the surface so that their scattering properties are independent, then the spectrum will be an average of a bright (methane) spectrum and a dark continuum spectrum and the methane absorption features will no longer be diminished by the continuum absorber. The primary goal of this analysis was to explain the newly discovered phase variation of the spectrum. Other models were not investigated at this time for this reason and because there is no other information yet available to help distinguish between them.

It is important to remember that the current spot model does not explain the secular dimming of Pluto. One suggestion (Cruikshank and Silvaggio 1980) proposes a net evaporation of methane from the surface over the past 35 years. The structure of the 8900-Å band shown in Fig. 4 may be related to this net evaporation. The double absorption peak seen in the spectrum of Fink *et al.* (1980), verified by Apt *et al.* (1983), is not seen in the 1983 data. This indicates that the physical characteristics of the methane could have changed during only one year. Interpretation of this change is difficult because of the lack of appropriate laboratory spectra, but the phenomena of increased band structure with decreasing temperature and phase changes in solid methane has been reported by Fink and Sill (1978). This is consistent with the fact that

Pluto is still approaching perihelion and therefore its mean temperature should be slowly increasing. Not enough is known about methane on Pluto to understand this behavior fully now. Further observations are required as Pluto passes through perihelion and begins to move away from the Sun.

The absorption coefficients used for the frost were approximated by measurements of liquid methane. Measurements of the absorption coefficients for the solid will improve the spectroscopic model. Details of the band shapes could be relied upon if a laboratory comparison can be made. For the same reason it would be useful to have methane gas absorption coefficients measured at Plutonian temperatures (40 to 60°K). The gas measurements would be more difficult to obtain because of the low vapor pressure of methane at those low temperatures but would aid in separating the frost and gas contributions to the spectrum of Pluto.

Despite the shortcomings of the current model, the strong presence of solid methane in the observed spectrum of Pluto can no longer be denied. The quantitative aspect of the model presented here will be greatly aided by improved physical parameters. The series of mutual eclipses between Pluto and Charon that has commenced (Binzel *et al.* 1985) will do much to increase our knowledge of the system.

ACKNOWLEDGMENTS

We thank M. A. DiSanti, F. Vilas, and J. R. Johnson for assisting with the observations and R. F. Poppen for assistance with the computer reductions. The observations and analysis of this work were supported by NASA Grant NSG 7070 while at the University of Arizona. The preparation and submission were supported by NASA Grant NGL 12-001-057 at the University of Hawaii.

REFERENCES

- ANDERSSON, L. E., AND J. D. FIX 1973. Pluto: New photometry and a determination of the axis of rotation. *Icarus* **20**, 279–283.
- APT, J., N. P. CARLETON, AND C. D. MACKAY 1983. Methane on Triton and Pluto: New CCD spectra. *Astrophys. J.* **270**, 342–350.
- ARVSEN, J. C., R. N. GRIFFIN, JR., AND B. D. PEARSON, JR. 1969. Determination of extraterrestrial so-

- lar spectral irradiance from a research aircraft. *Appl. Opt.* **8**, 2215–2232.
- BENNER, D. C. 1979. *The Visual and Near Infrared Spectrum of Methane and Its Application to Uranus, Neptune, Triton and Pluto*. Ph.D. thesis, University of Arizona, Tucson.
- BINZEL, R. P., AND J. D. MULHOLLAND 1984. Photometry of Pluto during the 1983 opposition: A new determination of the phase coefficient. *Astron. J.* **89**, 1759–1761.
- BINZEL, R. P., D. J. THOLEN, E. F. TEDESCO, B. J. BURATTI, AND R. M. NELSON 1985. The detection of eclipses in the Pluto–Charon system. *Science* **228**, 1193–1195.
- BRACEWELL, R. 1965. *The Fourier Transform and Its Applications*. McGraw–Hill, New York.
- BUIE, M. W. 1984. *Lightcurve CCD Spectrophotometry of Pluto*. Ph.D. thesis, University of Arizona, Tucson.
- CLARK, R. N., AND T. L. ROUSH 1984. Reflectance spectroscopy: Quantitative analysis techniques for remote sensing applications. *J. Geophys. Res.* **89**, 6239–6340.
- CRUIKSHANK, D. P., C. B. PILCHER, AND D. MORRISON 1976. Pluto: Evidence for methane frost. *Science* **194**, 835–837.
- CRUIKSHANK, D. P., AND P. M. SILVAGGIO 1980. The surface and atmosphere of Pluto. *Icarus* **41**, 96–102.
- DAVIES, M. E., V. K. ABALAKIN, C. A. CROSS, R. L. DUNCOMBE, H. MASURSKY, B. MORANDO, T. C. OWEN, P. K. SEIDELMANN, A. T. SINCLAIR, G. A. WILKINS, AND Y. S. TJUFLIN 1980. Report of the IAU Working Group on cartographic coordinates and rotational elements of the planets and satellites. *Celestial Mechanics* **22**, 205–230.
- FINK, U., D. C. BENNER, AND K. A. DICK 1977. Band model analysis of laboratory methane absorption spectra from 4500 to 10500 Å. *J. Quant. Spectrosc. Radiat. Transfer* **18**, 447–457.
- FINK, U., AND G. T. SILL 1978. The infrared spectral properties of frozen volatiles. In *Comets* (L. Wilkening, Ed.), pp. 164–202. Univ. of Arizona Press, Tucson.
- FINK, U., B. A. SMITH, D. C. BENNER, J. R. JOHNSON, H. J. REITSEMA, AND J. A. WESTPHAL 1980. Detection of a CH₄ atmosphere on Pluto. *Icarus* **44**, 62–71.
- HAPKE, B. 1981. Bidirectional reflectance spectroscopy. I. Theory. *J. Geophys. Res.* **86**, 3039–3054.
- HARDIE, R. H. 1965. A re-examination of the light variation of Pluto. *Astron. J.* **70**, 140.
- HEGE, E. K., E. N. HUBBARD, J. D. DRUMMOND, P. A. STRITTMATTER, AND S. P. WORDEN 1982. Speckle interferometric observations of Pluto and Charon. *Icarus* **50**, 72–81.
- JOHNSON, H. L. 1980. The absolute calibration of stellar spectrophotometry. *Rev. Mexicana Astron. Astrofis.* **5**, 25–30.
- JOHNSON, J. R., U. FINK, AND S. M. LARSON 1984. Charge couple device (CCD) spectroscopy of comets: Tuttle, Stephan–Oterma, Brooks 2, and Bowell. *Icarus* **60**, 351–372.
- LACIS, A. A., AND J. D. FIX 1972. An analysis of the light curve of Pluto. *Astrophys. J.* **174**, 449–453.
- MARCIALIS, R. L. 1983. *A Two-Spot Model for the Surface of Pluto*. M.S. thesis, Vanderbilt University, Nashville, TN.
- MARCOUX, J. E. 1969. Indices of refraction of some gasses in the liquid and solid state. *J. Opt. Soc. Amer.* **59**, 998.
- MORRISON, D., T. J. JONES, D. P. CRUIKSHANK, AND R. E. MURPHY 1975. The two faces of Iapetus. *Icarus* **24**, 157–171.
- NEFF, J. S., W. A. LANE, AND J. D. FIX 1974. An investigation of the rotational period of the planet Pluto. *Publ. Astron. Soc. Pacific* **86**, 225–230.
- RAMAPRASAD, K. R., J. CALDWELL, AND D. S. MCCLURE 1978. The vibrational overtone spectrum of liquid methane in the visible and near infrared: Applications to planetary studies. *Icarus* **35**, 400–409.
- SMITH, B. A., L. SODERBLUM, R. BATSON, P. BRIDGES, J. INGE, H. MASURSKY, E. SHOEMAKER, R. BEEBE, J. BOYCE, G. BRIGGS, A. BUNKER, S. A. COLLINS, C. J. HANSEN, T. V. JOHNSON, J. L. MITCHELL, R. J. TERRILE, A. F. COOK II, J. CUZZI, J. B. POLLACK, G. E. DANIELSON, A. P. INGERSOLL, M. E. DAVIES, G. E. HUNT, D. MORRISON, T. OWEN, C. SAGAN, J. VEVERKA, R. STROM, AND V. SUOMI 1982. A new look at the Saturn system: The Voyager 2 images. *Science* **215**, 504–537.
- SOIFER, B. T., G. NEUGEBAUER, AND K. MATTHEWS 1980. The 1.5–2.5 μm spectrum of Pluto. *Astron. J.* **85**, 166–167.
- STERN, S. A., AND L. TRAFTON 1984. Constraints on bulk composition, seasonal variation, and global dynamics of Pluto's atmosphere. *Icarus* **57**, 231–240.
- STROUD, A. H., AND D. SECREST 1966. *Gaussian Quadrature Formulas*. Prentice–Hall, Englewood Cliffs, NJ.
- THOLEN, D. J., AND E. F. TEDESCO 1986. *Pluto's Lightcurve: Results from Four Apparitions*. To be submitted for publication.
- TRAFTON, L. 1980. Does Pluto have a substantial atmosphere? *Icarus* **44**, 53–61.
- TRAFTON, L., AND S. A. STERN 1983. On the global distribution of Pluto's atmosphere. *Astrophys. J.* **267**, 872–881.
- WALKER, M. F., AND R. HARDIE 1955. A photometric determination of the rotational period of Pluto. *Publ. Astron. Soc. Pacific* **67**, 224–231.